



Quasi-Babinet principle in dielectric resonators and Mie voids

Masoud Hamidi ¹, Kirill Koshelev ^{2,*}, Sergei Gladyshev ¹, Adrià Canós Valero ¹,
Mario Hentschel ³, Harald Giessen ³, Yuri Kivshar ² and Thomas Weiss^{1,3,†}

¹*Institute of Physics, University of Graz, and NAWI Graz, Universitätsplatz 5, Graz 8010, Austria*

²*Nonlinear Physics Center, Research School of Physics, Australian National University, Canberra, ACT 2601, Australia*

³*4th Physics Institute and SCoPE, University of Stuttgart, Pfaffenwaldring 57, 70569, Stuttgart, Germany*



(Received 13 December 2023; revised 27 June 2024; accepted 12 November 2024; published 6 February 2025)

Advancing resonant nanophotonics requires novel building blocks. Recently, cavities in high-index dielectrics have been shown to resonantly confine light inside a lower-index region. These so-called Mie voids represent a counterpart to solid high-index dielectric Mie resonators, offering novel functionality such as resonant behavior in the ultraviolet spectral region. However, the well-known and highly useful Babinet's principle, which relates the scattering of solid and inverse structures, is not strictly applicable for this dielectric case as it is only valid for infinitesimally thin perfect electric conductors. Here, we show that Babinet's principle can be generalized to dielectric and magnetodielectric systems within certain boundaries, which we refer to as the quasi-Babinet principle and demonstrate for spherical and more generically shaped Mie resonators. Limitations arise due to geometry-dependent terms as well as material frequency dispersion and losses. Thus, our work not only offers deeper physical insight into the working mechanism of these systems but also establishes simple design rules for constructing dielectric resonators with complex functionalities from their complementary counterparts.

DOI: [10.1103/PhysRevResearch.7.013136](https://doi.org/10.1103/PhysRevResearch.7.013136)

I. INTRODUCTION

Babinet's principle is a fundamental concept in electromagnetism that relates the scattering properties of thin perfect metallic conductors to complementary apertures in metal sheets [1]. In optics, it applies to diffraction patterns from radiation passing through complementary metallic screens, exchanging transmission and reflection spectra [2]. The generalized form of Babinet's principle approximates the relation between transmission and reflection from flat absorbing scatterers and complementary apertures in absorbing media [3].

In the early 2000s, Babinet's principle was reformulated as a connection between the electric and magnetic fields of transverse electric (TE) and transverse magnetic (TM) modes of normal and inverted plasmonic structures, respectively [4,5]. In this form, it was applied for the design of plasmonic metamaterials and metasurfaces [6–9], leading to the concept of self-complementary metasurfaces [10–16], double negative index materials [17], manipulating polarization [18], enabling topological properties [19,20], wavefront control [21], filtering [22], coherent perfect absorption [23], observing plasmonic electromagnetically induced transparency [24,25], magnetic near-field imaging [26], and simultaneously realizing magnetic and electric hotspots [27].

Dielectric metaphotonics emerged recently as a promising alternative to plasmonics, featuring high-index dielectric

and semiconductor nanoresonators supporting geometrical Mie resonances as building blocks of photonic structures [28,29]. Mie resonances can be engineered in individual nanoresonators or their arrays in the form of metasurfaces and photonic crystal slabs [30], manifesting themselves as local and nonlocal modes, associated with bound states in the continuum [31,32], anapoles [33,34], and directional scattering [35].

Very recently, the concept of Mie voids was proposed in dielectric metaphotonics [36]. Counterintuitively, it was found that low-index materials inside a high-index environment, such as air voids in silicon or van der Waals 2D materials [37], can support Mie resonances in the infrared, visible, and even ultraviolet range due to confinement of light inside the air region, generalizing earlier works related to similar phenomena in low-index structures [38–41]. It was also shown that such Mie void modes are robust to geometrical and environmental changes, so that these modes can be realized experimentally by bringing the voids to the surface of thick silicon wafers. Unlike photonic crystal slabs and membranes relying on collective lattice resonances [42], even single Mie voids can function as individual pixels with highly localized resonant properties. In particular, voids exhibit pronounced scattering features, generating bright, high-resolution naturalistic colors [36].

In this Letter, we study the similarities and differences of Mie modes in voids and high-index nanoresonators. We reveal that for spherical nanoparticles, a quasi-Babinet principle can be established, connecting the electric and magnetic fields of a structure and its complementary counterpart, as well as their resonant frequencies and quality factors. The new principle holds quantitatively for voids (nanoparticles) with size larger than the wavelength, and approximately for sub-wavelength voids (nanoparticles). In structures with magnetic

*Contact author: kirill.koshelev@anu.edu.au

†Contact author: thomas.weiss@uni-graz.at

material response, the principle establishes a correspondence between resonant response of magnetodielectric particles and epsilon- and mu-near-zero particles. The quasi-Babinet principle remains approximately valid for nonspherical geometries, except in the vicinity of an avoided resonance crossing. Finally, we calculate the mode parameters for realistic dielectric materials with material losses in the near-infrared, visible, and ultraviolet spectral range, and demonstrate that the Babinet's principle is not applicable in the regions of high absorption and high dispersion, as intuitively expected.

Whenever applicable, the quasi-Babinet principle has remarkable similarities to the established Babinet principle between metallic films and their inverse counterparts: The resonance frequencies can be clearly mapped from one to the other, while the role of incident polarizations and resonant near fields is swapped. The former turns out to be very useful in determining the resonance frequencies of Mie voids. Although the task to find resonances in inverse structures seems to be straight-forward in numerical calculations, we have figured out that, without a good guess value as a start, it is challenging to obtain resonances where the fields are localized inside the voids. Most numerical schemes seem to preferentially find resonances with fields localized in the high-index surrounding. Moreover, it is important to highlight that in this work, we consider an open resonator. As a result, the established concepts of bound modes is no longer applicable, requiring a reformulation of the theory [43].

Yet, there are distinct differences between the quasi-Babinet principle and its established counterpart for metals: For the quasi-Babinet principle, the relation between resonances in the normal and inverse system is not given by the vacuum wavenumber, but by the wavenumber in the resonator medium, i.e., low-index medium for the voids and high-index medium in normal resonators. Equivalently, one can scale the size of the void by the ratio between high and low index to work at the same vacuum wavenumbers. Moreover, the geometrical relation between normal and inverse structure is truly three-dimensional for the quasi-Babinet principle. For the transition from a normal to the inverse structure consisting of two materials, this means that we need to keep the geometry same and swap the media, i.e., a low index becomes a high index and vice versa. In contrast, the Babinet principle for metals requires exchanging materials only in an ideally infinitely thin layer.

II. SPHERICAL GEOMETRY

As an analytically solvable example, we consider two complementary dielectric structures schematically shown in Figs. 1(a) and 1(b): a high-index sphere with internal refractive index n_i immersed in a low-index host medium with the refractive index $n_e \ll n_i$ and a low-index void in a high-index host medium with $n_e \gg n_i$. We study the applicability of Babinet's principle for these two scenarios. In the following, we use the term "normal structures" referring to dielectric particles, and "inverse structures" when referring to the voids embedded in a dielectric medium.

We start by calculating the plane wave total and partial multipolar scattering cross-sections for a normal sphere with $n_i = 4$, $n_e = 1$, $R = 75$ nm, and an inverse sphere with

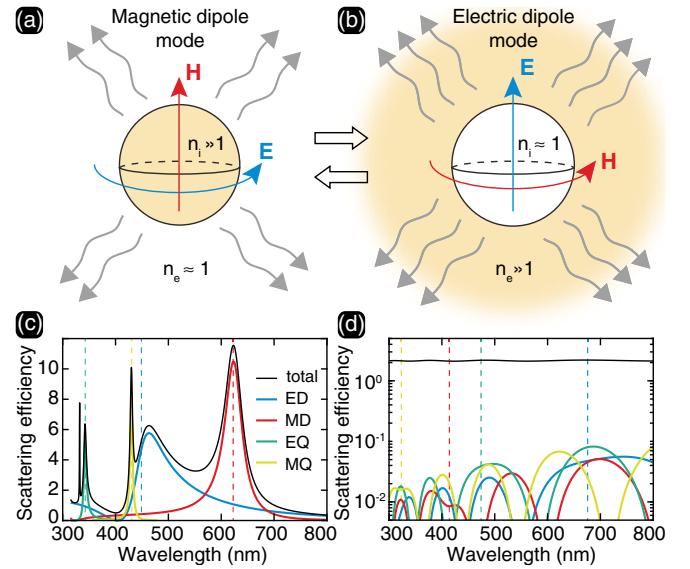


FIG. 1. Quasi-Babinet principle establishes a correspondence between mode properties of (a) a high-index dielectric structure and (b) a low-index void in high-index dielectric host medium as its inverse system. This principle connects modes of orthogonal polarizations, such as a magnetic dipole and an electric dipole Mie mode with their electric and magnetic fields, \mathbf{E} and \mathbf{H} (schematically displayed by blue and red arrows), respectively. (c), (d) Normalized plane wave scattering efficiency for (c) a spherical particle with $n_i = 4$, $n_e = 1$, $R = 75$ nm, and (d) a spherical void with $n_i = 1$, $n_e = 4$, $R = 300$ nm. Partial multipolar scattering components are shown with colors. Vertical dashed lines denote the resonant wavelengths of fundamental modes with $s = 1$ from Figs. 2(a) and 2(c).

$n_i = 1$, $n_e = 4$, $R = 300$ nm, shown in Figs. 1(c) and 1(d), respectively. The wavelength range is from 300 to 800 nm, corresponding to the same range of wavenumbers $\text{Re}(n_i k_0 R)$, defined further. Partial electric dipolar (ED), magnetic dipolar (MD), electric quadrupolar (EQ), and magnetic quadrupolar (MQ) scattering cross-sections normalized on the sphere geometrical cross-section are shown with line color. Vertical dashed lines denote the resonant wavelengths of fundamental modes, discussed further in Fig. 2. We can see that for normal structures the scattering peaks correspond to the individual modes, and their multipolar content matches the scattering multipoles. For the inverse structure, the total scattering is smeared out and the multipolar features do not correspond to the resonant mode positions. The latter effect can be explained by the effect of strong nonresonant scattering in voids.

Therefore, we approach the problem by investigating the behavior of the eigenmodes supported by the normal and inverse structures. Mie theory [36,44] yields the complex resonant wavenumbers $k_0 = \omega/c$ for the normal and inverse cases for TM and TE polarizations, as solutions to the following transcendental equations:

$$\text{TM modes: } \frac{\psi'_l(n_i k_0 R)}{\psi_l(n_i k_0 R)} = \frac{n_i \xi'_l(n_e k_0 R)}{n_e \xi_l(n_e k_0 R)}, \quad (1)$$

$$\text{TE modes: } \frac{\psi'_l(n_i k_0 R)}{\psi_l(n_i k_0 R)} = \frac{n_e \xi'_l(n_e k_0 R)}{n_i \xi_l(n_e k_0 R)}. \quad (2)$$

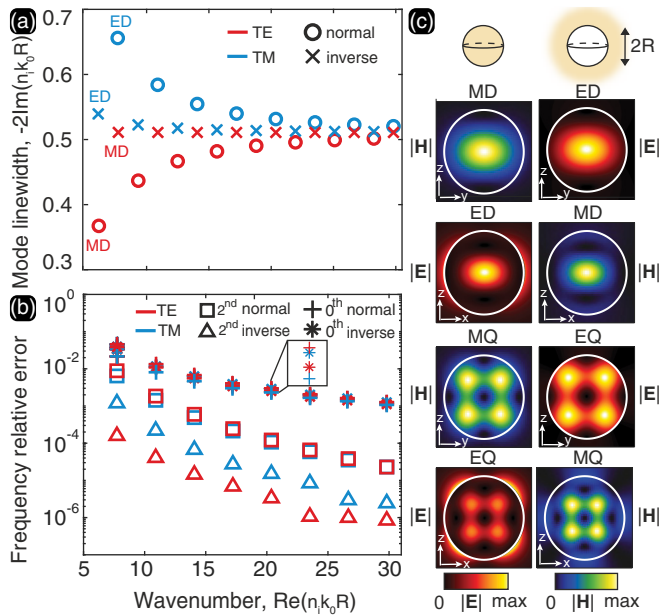


FIG. 2. Demonstration of the quasi-Babinet principle for a high-index dielectric sphere with $n_i = 4$, $n_e = 1$ and a spherical low-index void with $n_i = 1$, $n_e = 4$. (a) Mode wavenumber $\text{Re}(n_i k_0 R)$ vs mode linewidth $-2\text{Im}(n_i k_0 R)$ for $l = 1$ obtained via solving Eqs. (1) and (2). (b) Relative error $|1 - z_{ls}/z_{ls}^{\text{ana}}|$ between the approximate solution z_{ls} of Eqs. (3) and (4) for different orders of approximation and z_{ls}^{ana} as solutions of Eqs. (1) and (2) for $l = 1$. (c) Field profiles in normal and inverse structures for the fundamental MD and ED modes ($s = 1$, $l = 1$, $m = 1$) labeled in (a) and fundamental MQ and EQ modes ($s = 1$, $l = 2$, $m = 1$).

Here, $l = 1, 2, \dots$, is the orbital mode index, and n_e and n_i are the refractive indices outside and inside the sphere with radius R , respectively. The prime denotes derivatives with respect to the argument, and ψ_l as well as ξ_l are the Riccati-Bessel functions of order l , with $\psi_l(x) = x j_l(x)$ and $\xi_l(x) = x h_l(x)$, where j_l and h_l are the spherical Bessel and outgoing spherical Hankel functions, respectively. We note that the modes of spherical particles are degenerate with respect to the azimuthal index $m = 0, \pm 1, \dots, \pm l$.

We can expand the left and right part of Eqs. (1) and (2) in a series with respect to $1/z$ for $z = n_i k_0 R$, assuming $k_0 R \gg 1$, and solve the equation up to a specific order of $1/z$. For high-contrast normal ($n_e \ll n_i$) and high-contrast inverse ($n_e \gg n_i$) structures, the solutions up to second order are (see Sec. I A in the SM [45])

$$z_{ls} \approx \tilde{z}_{l+1,s} - \frac{\beta_l}{\tilde{z}_{l+1,s}} \mp i \frac{n_i}{n_e} \frac{\beta_l}{\tilde{z}_{l+1,s}^2}, \quad \text{for } \begin{cases} \text{TM normal} \\ \text{TE inverse} \end{cases}, \quad (3)$$

$$z_{ls} \approx \tilde{z}_{ls} - \frac{\beta_l}{\tilde{z}_{ls}} \pm i \frac{n_i}{n_e} \frac{\beta_l}{\tilde{z}_{ls}^2}, \quad \text{for } \begin{cases} \text{TE normal} \\ \text{TM inverse} \end{cases}. \quad (4)$$

Here, $s = 1, 2, \dots$, is the radial mode index, $\beta_l = l(l+1)/2$, and $\tilde{z}_{ls} = \pi(s + (l-1)/2) - i \arctanh(n_{<}/n_{>})$ as the zeroth order solution for $n_{<}$ and $n_{>}$ is the lowest and highest refractive index, respectively. We note the expansion up to \tilde{z}_{ls} was known in the literature [46], but without acknowledging the similarities between normal and inverse structures.

The comparison of TM (TE) modes of normal structures and TE (TM) modes of inverse structure reveals that the solutions are identical up to the first order of $1/z$. The difference in resonant wavenumbers of complementary modes is given by the second-order correction. We denote this approximate correspondence as the quasi-Babinet principle. As a result of it, we will show that the modes of the complementary structures feature very similar resonant wavenumbers, but different linewidths. For comparison, we show that for a one-dimensional planar dielectric slab and complementary air slot slab the exact Babinet principle holds (see Sec. I B in [45, Sec. IB]).

Next, we evaluate the validity of the quasi-Babinet principle numerically by comparing solutions z_{ls}^{ana} of Eqs. (1) and (2) for normal ($n_i = 4$, $n_e = 1$) and inverse ($n_i = 1$, $n_e = 4$) cases, corresponding to a silicon sphere in air and an air void in silicon in the near-infrared range, respectively. For solving the transcendental Eqs. (1) and (2), we used a custom Python code. Figure 2(a) depicts the mode linewidth with respect to the real part of resonant wavenumbers for modes with $l = 1$ and $m = 1$ that can be excited with a plane wave. The difference between the real part of $n_i k_0 R$ for normal TE (TM) and inverse TM (TE) modes is small and decreases with the increase of the radial mode index s (from left to right). The difference between the linewidths of complementary modes is larger, but also decreases with the increase of the radial mode index. Therefore, the quasi-Babinet principle accuracy increases with the increase of s .

To quantify the validity of the approximate solutions in Eqs. (3) and (4), we calculated the relative error $|1 - z_{ls}/z_{ls}^{\text{ana}}|$ between the analytical wavenumbers z_{ls}^{ana} and the approximate zeroth- and second-order solutions z_{ls} for both the normal and inverse cases, shown in Fig. 2(b). The inverse TE modes (red triangles) exhibits the highest accuracy for the second-order solution compared to the other cases. We note Fig. 2(b) confirms that the zeroth-order solution can be used to predict the location of the real part of the resonant wavenumbers.

Figure 2(c) displays the absolute value of the electric field \mathbf{E} and magnetic field \mathbf{H} for the lowest-order multipolar modes of the normal and inverse structures with $m = 1$ normalized to their maximum values, which are MD and ED modes with $s = 1$, $l = 1$ and MQ and EQ modes with $s = 1$, $l = 2$. Close resemblance between the fields of the normal structure modes and the corresponding modes of the void structure confirms the validity of the quasi-Babinet principle.

III. MAGNETODIELECTRIC MATERIALS

We further investigate the validity of the quasi-Babinet principle for magnetodielectric spherical structures with nonzero permeability and permittivity contrast (for more details see SM [45]). In this case, “normal” and “inverse” structures are defined with respect to the relative values of the impedance, $Z_{i,e}$, and refractive index, $n_{i,e}$, between the internal and external domains of the resonator.

In our example, we consider two complementary magnetodielectric structures: a high-index low-impedance sphere with n_i , Z_i inside immersed in a low-index high-impedance host medium with $n_e \ll n_i$, $Z_e \gg Z_i$, and a low-index high-impedance void in a high-index low-impedance host medium

with $n_e \gg n_i$, $Z_e \ll Z_i$. The equations for complex mode frequencies can be written as transcendental equations similar to Eqs. (1) and (2):

$$\text{TM modes: } \frac{\psi'_l(n_i k_0 R)}{\psi_l(n_i k_0 R)} = \frac{Z_e \xi'_l(n_e k_0 R)}{Z_i \xi_l(n_e k_0 R)}, \quad (5)$$

$$\text{TE modes: } \frac{\psi'_l(n_i k_0 R)}{\psi_l(n_i k_0 R)} = \frac{Z_i \xi'_l(n_e k_0 R)}{Z_e \xi_l(n_e k_0 R)}. \quad (6)$$

Following the procedure used to derive Eqs. (3) and (4), we expand the left and right part of Eqs. (5) and (6) in a series with respect to $1/z$ for $z = n_i k_0 R$, assuming $k_0 R \gg 1$, and solve the equation up to a specific order of $1/z$. For high-contrast normal ($n_e \ll n_i$, $Z_e \gg Z_i$) and high-contrast inverse ($n_e \gg n_i$, $Z_e \ll Z_i$) structures, the solutions up to second order are (see Sec. II in the SM [45])

$$z_{ls} \approx \tilde{z}_{l+1,s} - \frac{\beta_l}{\tilde{z}_{l+1,s}} - i \frac{Z_e \mu_i^2 \beta_l}{Z_i \mu_e^2 \tilde{z}_{l+1,s}^2}, \quad \text{for TM normal,} \quad (7)$$

$$z_{ls} \approx \tilde{z}_{l+1,s} - \frac{\beta_l}{\tilde{z}_{l+1,s}} + i \frac{Z_e \beta_l}{Z_i \tilde{z}_{l+1,s}^2}, \quad \text{for TE inverse,} \quad (8)$$

$$z_{ls} \approx \tilde{z}_{ls} - \frac{\beta_l}{\tilde{z}_{ls}} + i \frac{Z_e \mu_i^2 \beta_l}{Z_i \mu_e^2 \tilde{z}_{ls}^2} \quad \text{for TE normal,} \quad (9)$$

$$z_{ls} \approx \tilde{z}_{ls} - \frac{\beta_l}{\tilde{z}_{ls}} - i \frac{Z_e \beta_l}{Z_i \tilde{z}_{ls}^2} \quad \text{for TM inverse.} \quad (10)$$

Here, $\mu_i = n_i Z_i$, $\mu_e = n_e Z_e$ are internal and external permeabilities, respectively, and $\tilde{z}_{ls} = \pi(s + (l-1)/2) - i \arctan(Z_-/Z_+)$ is the zeroth order solution for Z_- and Z_+ as the lowest and highest impedance, respectively. We can see that Eqs. (7)–(10) transform to Eqs. (3) and (4) for nonmagnetic materials with $\mu_i = \mu_e = 1$.

After establishing the quasi-Babinet principle for magnetodielectric materials, we compare it with the electromagnetic duality [47]. We illustrate both transformations in Fig. 3 as a correspondence between relative permeabilities, μ_i/μ_e , and permittivities, $\varepsilon_i/\varepsilon_e$, where the latter are given by $\varepsilon_i = n_i/Z_i$, $\varepsilon_e = n_e/Z_e$.

The duality principle corresponds to the transformation $Z_i \rightarrow Z_e$, $Z_e \rightarrow Z_i$. We note that duality provides an exact TE-TM correspondence via the transformation of Eq. (5) into Eq. (6) and visa versa. In terms of relative permeabilities and permittivities, the duality corresponds to

$$\frac{\varepsilon_i}{\varepsilon_e} \rightarrow \frac{\mu_i}{\mu_e}, \quad \frac{\mu_i}{\mu_e} \rightarrow \frac{\varepsilon_i}{\varepsilon_e}. \quad (11)$$

The correspondence via electromagnetic duality, Eq. (11), is shown schematically in Fig. 3(a) with a solid orange line for a dielectric particle (point A) with $\varepsilon_i/\varepsilon_e > 1$, $\mu_i/\mu_e = 1$ and a magnetic particle (point B) with $\mu_i/\mu_e > 1$, $\varepsilon_i/\varepsilon_e = 1$.

The quasi-Babinet principle corresponds to simultaneous transformations $Z_i \rightarrow Z_e$, $Z_e \rightarrow Z_i$ and $n_i \rightarrow n_e$, $n_e \rightarrow n_i$. As discussed before, the quasi-Babinet principle establishes an approximate TE-TM correspondence between modes of normal and inverse structures up to its applicability range. In terms of relative permeabilities and permittivities, the quasi-Babinet principle establishes

$$\frac{\varepsilon_i}{\varepsilon_e} \rightarrow \left(\frac{\varepsilon_i}{\varepsilon_e} \right)^{-1}, \quad \frac{\mu_i}{\mu_e} \rightarrow \left(\frac{\mu_i}{\mu_e} \right)^{-1}. \quad (12)$$

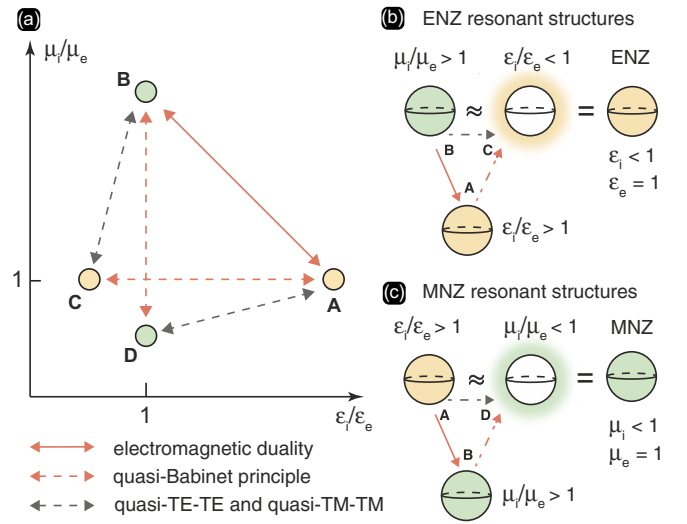


FIG. 3. Electromagnetic duality, quasi-Babinet principle and epsilon-near-zero and mu-near-zero materials in magneto-dielectric materials. (a) Correspondence between relative permeabilities and permittivities of normal and inverse structures via the electromagnetic duality (solid orange line), the quasi-Babinet principle (dashed orange line), and their combination giving a quasi-TE-TE and quasi-TM-TM correspondence (dashed gray line). (b) and (c) Schematic relation of quasi-TE-TE and quasi-TM-TM correspondence to (b) epsilon-near-zero (ENZ) and (c) mu-near-zero (MNZ) resonant structures.

The correspondence via the quasi-Babinet principle, Eq. (12), is shown schematically in Fig. 3(a) with dashed orange lines for a dielectric particle (point A) with $\varepsilon_i/\varepsilon_e > 1$, $\mu_i/\mu_e = 1$ and a dielectric void (point C) with $\varepsilon_i/\varepsilon_e < 1$, $\mu_i/\mu_e = 1$. The same correspondence can be established for a magnetic particle (point B) with $\mu_i/\mu_e > 1$, $\varepsilon_i/\varepsilon_e = 1$ and a magnetic void (point D) with $\mu_i/\mu_e < 1$, $\varepsilon_i/\varepsilon_e = 1$.

We can then combine the transformations in Eqs. (11) and (12) and establish a direct correspondence between the dielectric particle (point A) and magnetic void (point D), as well as the magnetic particle (point B) and dielectric void (point C), shown with a dashed gray line in Fig. 3(a). Such correspondences describe the transformation of TM modes given by Eq. (5) into TE modes, and TE modes given by Eq. (6) into TM modes via $n_i \rightarrow n_e$, $n_e \rightarrow n_i$, which can be written as

$$\frac{\varepsilon_i}{\varepsilon_e} \rightarrow \left(\frac{\mu_i}{\mu_e} \right)^{-1}, \quad \frac{\mu_i}{\mu_e} \rightarrow \left(\frac{\varepsilon_i}{\varepsilon_e} \right)^{-1}. \quad (13)$$

Therefore, we call these transformations as quasi-TM-TM and quasi-TE-TE correspondence, respectively.

The established quasi-TM-TM and quasi-TE-TE correspondence can be used to describe the mode properties of epsilon-near-zero (ENZ) and mu-near-zero-material (MNZ) resonant structures through the mode properties of normal dielectric and magnetic particles. This can be done by using the fact that electromagnetic response of a dielectric Mie void is equivalent to an ENZ particle, and of a magnetic Mie void is equivalent to an MNZ particle, as they are characterized by the same relative permeabilities and permittivities, $\varepsilon_i/\varepsilon_e$ and

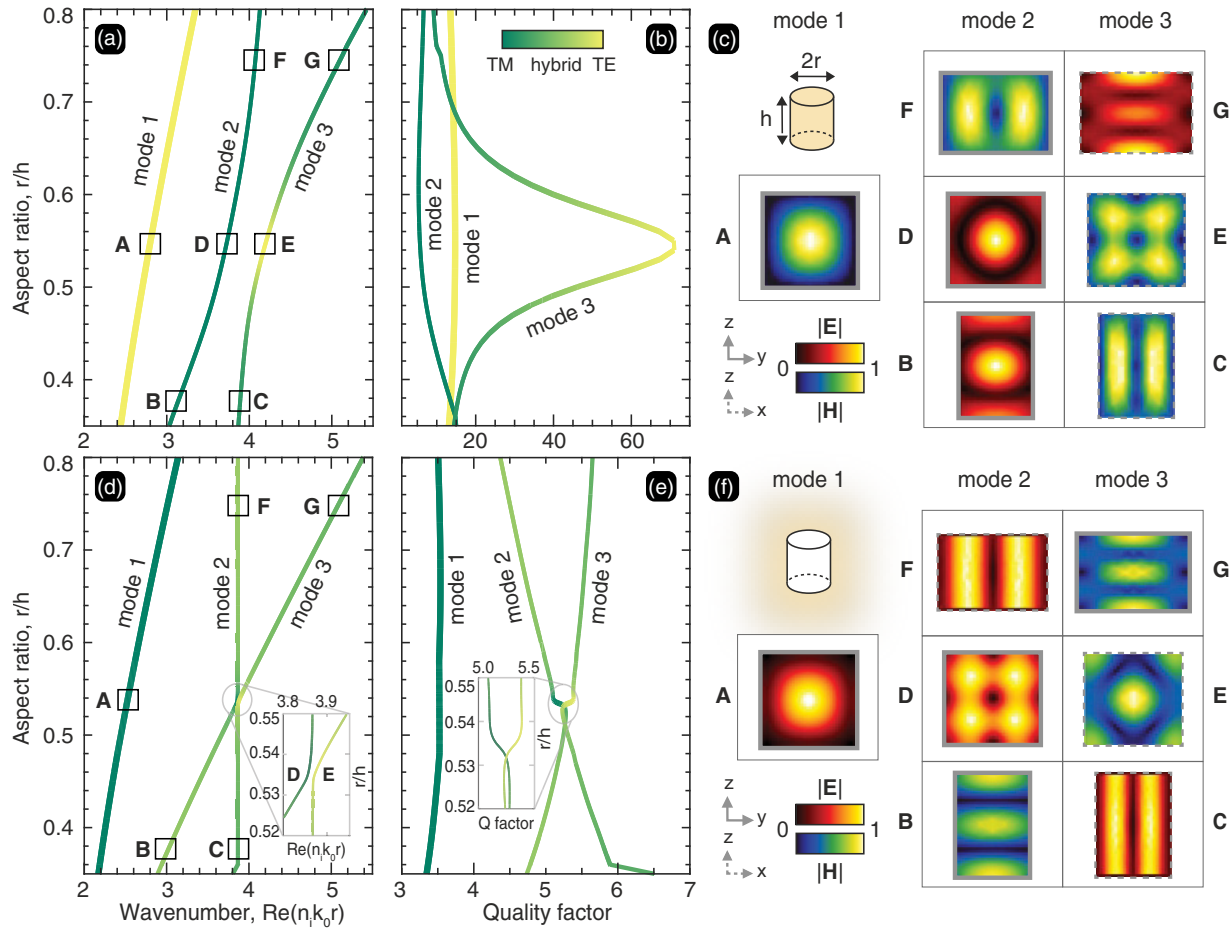


FIG. 4. Quasi-Babinet principle for cylinder-shaped resonators: Mode wavenumber, quality factor, and field profiles vs cylinder aspect ratio for the fundamental modes of (a)–(c) normal ($n_i = 4$, $n_e = 1$) and (d), (e) inverse structures ($n_i = 1$, $n_e = 4$), respectively. Only the eigenmodes that can be excited by a plane wave incident along the cylinder axis have been considered. The line color in (a), (b), (d), and (e) is defined by the mode’s far-field polarization degree. The insets display data within a narrow range of parameters near the avoided resonance crossing. The box line style in (c) and (f) denotes zy (solid) and zx (dashed) cross-sections.

μ_i/μ_e . Figures 3(b) and 3(c) show schematically the direct mode correspondence between a magnetic particle (point B) and an ENZ dielectric particle with $\epsilon_i/\epsilon_e < 1$, $\mu_i/\mu_e = 1$, as well as the direct mode correspondence between a dielectric particle (point A) and a MNZ particle with $\mu_i/\mu_e < 1$, $\epsilon_i/\epsilon_e = 1$.

We also note that the described relation between the electromagnetic duality, quasi-Babinet principle and quasi-TE-TE, quasi-TM-TM correspondences become approximate for nonspherical geometries and structures with material losses, with the same applicability range as the quasi-Babinet principle discussed below.

IV. NONSPHERICAL GEOMETRIES

We next analyze the Babinet conditions for a dielectric cylinder with $n_i = 4$ in air and a cylinder-shaped air void in an environment with $n_e = 4$ calculating their eigenmode spectrum. Figure 4 illustrates the mode wavenumber, quality factor, and field profiles of the first three fundamental modes of the normal and inverse cylinder structures with $m = 1$ as a function of the aspect ratio r/h of radius r and height h . For numerical calculations, we use the eigenmode solver in

COMSOL Multiphysics©. Unlike spheres, the eigenmodes of a cylinder have a mixed TE-TM character [48,49], which we characterize by performing the multipolar decomposition of the eigenmode’s radiated power into TE and TM contributions, which are then color-coded in Figs. 4(a), 4(b), 4(d), and 4(e) (see also Sec. III in the SM [45]). In general, the reason for the hybridization of eigenmodes is that they are characterized by the same irreducible representation and are close in resonance frequency [48].

The quasi-Babinet principle holds well for mode 1, with a relative difference in wavenumber values below 13% for the given range of r/h . Importantly, mode 1 exhibits a pure TE and TM nature for normal and inverse structures, respectively. The resonant frequencies of modes 2 and 3 avoid a crossing at $r/h \simeq 0.535$ showing a clear signature of mode coupling. In the normal structure, modal interference results in a decrease in the quality factor of mode 2, and a pronounced peak of the quality factor of mode 3, signaling the formation of a quasi-bound state in the continuum [50] of pure TE nature. In the inverse cylinder, the coupling between the modes is weaker and the peak in the quality factor is less pronounced, but still mode 3 becomes a pure TE mode. We note that the observed (small) increase of quality factor for mode 3 at $r/h \simeq 0.535$

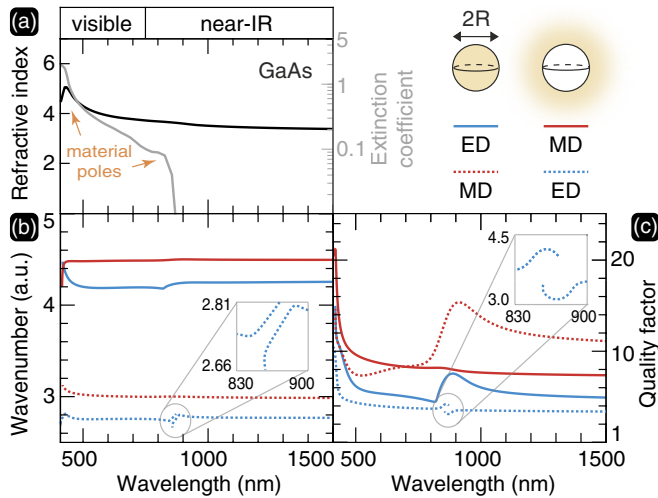


FIG. 5. (a)–(c) Effect of material absorption: Dependence of (a) material refractive index, (b) mode wavenumber $\text{Re}(n_i k_0 R)$, and (c) quality factor on resonant wavelength from the visible to near-infrared range for normal and inverse structures composed of air and GaAs. The upper right inset depicts the color legend for the ED and MD modes. The wavelengths of material poles are shown with brown arrows.

is the first demonstration of the formation of quasibound state in the continuum in individual void structures. Modes 2 and 3 are characterized by the E_{1u} irreducible representation in the normal structure, and by E_{1g} in the inverse one [48]. The field profiles for all modes at the avoided resonance crossing and away from it are displayed in Figs. 4(c) and 4(f). From the quality factor behavior and field profiles, we conclude that the quasi-Babinet principle still holds approximately for $r/h < 0.5$ and $r/h > 0.6$, i.e., when the hybrid modes are spectrally separated. We also show numerically that the quasi-Babinet principle holds for cubelike structures (see Sec. IV in the SM [45]).

V. EFFECT OF MATERIAL LOSSES

We next analyze how the material losses affect the range of applicability of the quasi-Babinet principle. We calculate the resonant frequencies of fundamental modes for normal ($n_i = n + ik$) and inverse ($n_e = n + ik$) spherical structures composed of air and GaAs with realistic dispersion. We use a custom Matlab code to solve Eqs. (1) and (2) with the material permittivity function extended to the complex frequency plane by fitting to several material poles (see Sec. V in the SM [45]). Figure 5 displays the material refractive index, mode wavenumber $\text{Re}(n_i k_0 R)$, quality factor for MD, and ED

modes of normal and inverse spherical resonators. Insets in Fig. 5(b) display a zoom into the spectral region, in which a material pole hybridizes with an optical resonance, resulting in two disconnected dispersion branches [51].

Figure 5 shows that the quasi-Babinet principle is valid for the low-loss range, and the complementary modes (normal ED with inverse MD, and normal MD with inverse ED) have very close wavenumbers. We see that in the range of high material losses as well as in the vicinity of material permittivity function poles, the quasi-Babinet correspondence breaks down. To understand the underlying reason, we analyze how the absorption losses change the mode eigenfrequency for normal and inverse structures using the zeroth-order analytical expression in Eqs. (3) and (4) (see Sec. VI in the SM [45]). We find that, while the modes of the normal structure are affected by the losses in the whole particle volume, the modes of inverse structures are naturally less sensitive, since their fields are primarily localized in air.

VI. CONCLUSION

We have established a quasi-Babinet principle that allows us to predict mode characteristics of dielectric Mie voids from dielectric Mie resonators and vice versa. We have determined analytically and numerically the applicability range of the quasi-Babinet principle depending on the spatial dimension, geometry, and material losses of the structure. We analyzed extension of this principle to magnetodielectric structures and its connection to epsilon-and-mu-near-zero photonics. We anticipate the developed principle to pave the way toward smart engineering of nanoscale metadevices comprising applications in strong light-matter interaction, biosensing, and quantum information processing.

ACKNOWLEDGMENTS

K.K. acknowledges Oleh Yermakov and Andrey Bogdanov for many useful comments and discussions. This work was supported by Bundesministerium für Bildung und Forschung, Deutsche Forschungsgemeinschaft, (SPP1839 “Tailored Disorder” and GRK2642 “Towards Graduate Experts in Photonic Quantum Technologies”), the Ministerium für Wissenschaft, Forschung und Kunst Baden-Württemberg (RiSC Project “Mie Voids”, ZAQuant).

M.H. and K.K. contributed equally to this work. K.K. and T.W. conceived the original idea. M.H., K.K., A.C.V., S.G., and T.W. performed the simulations and modeling. All authors discussed, interpreted, and corroborated the results. All authors participated in the preparation and writing of the manuscript. K.K. and T.W. supervised the work.

[1] J. Meixner, Das babinetsche prinzip der optik, *Z. Naturfors. A* **1**, 496 (1946).
 [2] H. G. Booker, Slot aerials and their relation to complementary wire aerials (Babinet’s principle), *J. Instit. Elect. Eng.-Part IIIA: Radiolocation* **93**, 620 (1946).

[3] H. Neugebauer, Extension of Babinet’s principle to absorbing and transparent materials, and approximate theory of backscattering by plane, absorbing disks, *J. Appl. Phys.* **28**, 302 (1957).
 [4] T. Zentgraf, T. P. Meyrath, A. Seidel, S. Kaiser, H. Giessen, C. Rockstuhl, and F. Lederer, Babinet’s principle for optical

- frequency metamaterials and nanoantennas, *Phys. Rev. B* **76**, 033407 (2007).
- [5] N. Liu, S. Kaiser, and H. Giessen, Magnetoinductive and electroinductive coupling in plasmonic metamaterial molecules, *Adv. Mater.* **20**, 4521 (2008).
- [6] F. Falcone, T. Lopetegi, M. A. G. Laso, J. D. Baena, J. Bonache, M. Beruete, R. Marqués, F. Martín, and M. Sorolla, Babinet principle applied to the design of metasurfaces and metamaterials, *Phys. Rev. Lett.* **93**, 197401 (2004).
- [7] I. Al-Naib, C. Jansen, and M. Koch, Applying the Babinet principle to asymmetric resonators, *Electron. Lett.* **44**, 1228 (2008).
- [8] J. Ortiz, J. del Risco, J. Baena, and R. Marqués, Extension of Babinet's principle for plasmonic metasurfaces, *Appl. Phys. Lett.* **119**, 161103 (2021).
- [9] J. D. Ortiz, J. D. Baena, R. Marqués, A. N. Enemuó, J. Gollub, R. Akhmechet, B. Penkov, C. Sarantos, and D. T. Crouse, Babinet's principle and saturation of the resonance frequency of scaled-down complementary metasurfaces, *Appl. Phys. Lett.* **118**, 221901 (2021).
- [10] R. Singh, C. Rockstuhl, C. Menzel, T. P. Meyrath, M. He, H. Giessen, F. Lederer, and W. Zhang, Spiral-type terahertz antennas and the manifestation of the mushroom principle, *Opt. Express* **17**, 9971 (2009).
- [11] Y. Nakata, Y. Urade, T. Nakanishi, and M. Kitano, Plane-wave scattering by self-complementary metasurfaces in terms of electromagnetic duality and Babinet's principle, *Phys. Rev. B* **88**, 205138 (2013).
- [12] J. D. Ortiz, J. D. Baena, V. Losada, F. Medina, R. Marques, and J. A. Quijano, Self-complementary metasurface for designing narrow band pass/stop filters, *IEEE microwave and wireless components Letters* **23**, 291 (2013).
- [13] D. González-Ovejero, E. Martini, and S. Maci, Surface waves supported by metasurfaces with self-complementary geometries, *IEEE Trans. Antennas Propag.* **63**, 250 (2014).
- [14] Y. Urade, Y. Nakata, T. Nakanishi, and M. Kitano, Frequency-independent response of self-complementary checkerboard screens, *Phys. Rev. Lett.* **114**, 237401 (2015).
- [15] J. D. Baena, J. P. del Risco, A. P. Slobozhanyuk, S. B. Glybovski, and P. A. Belov, Self-complementary metasurfaces for linear-to-circular polarization conversion, *Phys. Rev. B* **92**, 245413 (2015).
- [16] O. Yermakov, V. Lenets, A. Sayanskiy, J. Baena, E. Martini, S. Glybovski, and S. Maci, Surface waves on self-complementary metasurfaces: all-frequency hyperbolicity, extreme canalization, and TE-TM polarization degeneracy, *Phys. Rev. X* **11**, 031038 (2021).
- [17] L. Zhang, T. Koschny, and C. M. Soukoulis, Creating double negative index materials using the babinet principle with one metasurface, *Phys. Rev. B* **87**, 045101 (2013).
- [18] M. Zalkovskij, R. Malureanu, C. Kremers, D. N. Chigrin, A. Novitsky, S. Zhukovsky, P. T. Tang, P. U. Jepsen, and A. V. Lavrinenko, Optically active babinet planar metamaterial film for terahertz polarization manipulation, *Laser Photonics Rev.* **7**, 810 (2013).
- [19] J. B. Dia'aaldin and D. F. Sievenpiper, Guiding waves along an infinitesimal line between impedance surfaces, *Phys. Rev. Lett.* **119**, 106802 (2017).
- [20] D. J. Bisharat and D. F. Sievenpiper, Electromagnetic-dual metasurfaces for topological states along a 1d interface, *Laser Photonics Rev.* **13**, 1900126 (2019).
- [21] X. Ni, S. Ishii, A. V. Kildishev, and V. M. Shalaev, Ultra-thin, planar, Babinet-inverted plasmonic metalenses, *Light Sci. Appl.* **2**, e72 (2013).
- [22] Y. Urade, Y. Nakata, K. Okimura, T. Nakanishi, F. Miyamaru, M. W. Takeda, and M. Kitano, Dynamically Babinet-invertible metasurface: a capacitive-inductive reconfigurable filter for terahertz waves using vanadium-dioxide metal-insulator transition, *Opt. Express* **24**, 4405 (2016).
- [23] Y. Urade, Y. Nakata, T. Nakanishi, and M. Kitano, Broadband and energy-concentrating terahertz coherent perfect absorber based on a self-complementary metasurface, *Opt. Lett.* **41**, 4472 (2016).
- [24] N. Liu, T. Weiss, M. Mesch, L. Langguth, U. Eigenthaler, M. Hirscher, C. Sonnichsen, and H. Giessen, Planar metamaterial analogue of electromagnetically induced transparency for plasmonic sensing, *Nano Lett.* **10**, 1103 (2010).
- [25] M. Hentschel, T. Weiss, S. Bagheri, and H. Giessen, Babinet to the half: coupling of solid and inverse plasmonic structures, *Nano Lett.* **13**, 4428 (2013).
- [26] M. Horák, V. Křápek, M. Hrtoň, A. Konečná, F. Ligmajer, M. Stöger-Pollach, T. Šamořil, A. Paták, Z. Édes, O. Metelka *et al.*, Limits of Babinet's principle for solid and hollow plasmonic antennas, *Sci. Rep.* **9**, 4004 (2019).
- [27] M. Hrtoň, A. Konečná, M. Horák, T. Šikola, and V. Křápek, Plasmonic antennas with electric, magnetic, and electromagnetic hot spots based on Babinet's principle, *Phys. Rev. Appl.* **13**, 054045 (2020).
- [28] R. Won, Into the Mie-tronic'era, *Nat. Photonics* **13**, 585 (2019).
- [29] Y. Kivshar, The rise of Mie-tronics, *Nano Lett.* **22**, 3513 (2022).
- [30] K. Koshelev and Y. Kivshar, Dielectric resonant metaphotonics, *ACS Photonics* **8**, 102 (2021).
- [31] C. W. Hsu, B. Zhen, A. D. Stone, J. D. Joannopoulos, and M. Soljačić, Bound states in the continuum, *Nat. Rev. Mater.* **1**, 16048 (2016).
- [32] K. Koshelev, S. Lepeshov, M. Liu, A. Bogdanov, and Y. Kivshar, Asymmetric metasurfaces with high-Q resonances governed by bound states in the continuum, *Phys. Rev. Lett.* **121**, 193903 (2018).
- [33] A. E. Miroshnichenko, A. B. Evlyukhin, Y. F. Yu, R. M. Bakker, A. Chipouline, A. I. Kuznetsov, B. Luk'yanchuk, B. N. Chichkov, and Y. S. Kivshar, Nonradiating anapole modes in dielectric nanoparticles, *Nat. Commun.* **6**, 8069 (2015).
- [34] A. Canós Valero, E. A. Gurvitz, F. A. Benimetskiy, D. A. Pidgayko, A. Samusev, A. B. Evlyukhin, V. Bobrovs, D. Redka, M. I. Tribelsky, M. Rahmani *et al.*, Theory, observation, and ultrafast response of the hybrid anapole regime in light scattering, *Laser Photonics Rev.* **15**, 2100114 (2021).
- [35] W. Liu and Y. S. Kivshar, Generalized Kerker effects in nanophotonics and meta-optics, *Opt. Express* **26**, 13085 (2018).
- [36] M. Hentschel, K. Koshelev, F. Sterl, S. Both, J. Karst, L. Shamsafar, T. Weiss, Y. Kivshar, and H. Giessen, Dielectric Mie voids: confining light in air, *Light Sci. Appl.* **12**, 3 (2023).
- [37] A. Sarbajna, D. R. Danielsen, L. N. Casses, N. Stenger, P. Bøggild, and S. Raza, Encapsulated void resonators in lossy dielectric van der Waals heterostructures, *Laser Photon. Rev.* **19**, 2401215 (2024).

- [38] F. Kusunoki, T. Kohama, T. Hiroshima, S. Fukumoto, J. Takahara, and T. Kobayashi, Narrow-band thermal radiation with low directivity by resonant modes inside tungsten microcavities, *Jpn. J. Appl. Phys.* **43**, 5253 (2004).
- [39] A. S. Shalin, Broadband blooming of a medium modified by an incorporated layer of nanocavities, *JETP Lett.* **91**, 636 (2010).
- [40] V. R. Almeida, Q. Xu, C. A. Barrios, and M. Lipson, Guiding and confining light in void nanostructure, *Opt. Lett.* **29**, 1209 (2004).
- [41] C.-C. Chen, Electromagnetic resonances of immersed dielectric spheres, *IEEE Trans. Antennas Propag.* **46**, 1074 (1998).
- [42] M. Ossiander, M. L. Meretska, H. K. Hampel, S. W. D. Lim, N. Knefz, T. Jauk, F. Capasso, and M. Schultze, Extreme ultraviolet metalens by vacuum guiding, *Science* **380**, 59 (2023).
- [43] S. Both and T. Weiss, Resonant states and their role in nanophotonics, *Semicond. Sci. Technol.* **37**, 013002 (2022).
- [44] G. Mie, Beiträge zur Optik trüber Medien, speziell kolloidaler Metallösungen, *Ann. Phys.* **330**, 377 (1908).
- [45] See Supplemental Material at <http://link.aps.org/supplemental/10.1103/PhysRevResearch.7.013136> for the derivation of the analytical solution in Eqs. (3)–(10), derivation of the quasi-Babinet principle for magnetodielectric materials, multipolar decomposition for disk-shaped structures, numerical analysis of the quasi-Babinet principle for cubic structures, description of numerical procedure used for eigenmode analysis of dispersive structures, table containing numerical values of the material poles used for eigenmode analysis of the dispersive structures, and analysis of absorption losses effect on the quasi-Babinet principle, which includes Refs. [40,52–62].
- [46] Z. Sztranyovszky, W. Langbein, and E. A. Muljarov, Optical resonances in graded index spheres: A resonant-state-expansion study and analytic approximations, *Phys. Rev. A* **105**, 033522 (2022).
- [47] K. Y. Bliokh, A. Y. Bekshaev, and F. Nori, Dual electromagnetism: helicity, spin, momentum and angular momentum, *New J. Phys.* **15**, 033026 (2013).
- [48] S. Gladyshev, K. Frizyuk, and A. Bogdanov, Symmetry analysis and multipole classification of eigenmodes in electromagnetic resonators for engineering their optical properties, *Phys. Rev. B* **102**, 075103 (2020).
- [49] A. V. Kuznetsov, A. Canós Valero, H. K. Shamkhi, P. Terekhov, X. Ni, V. Bobrov, M. V. Rybin, and A. S. Shalin, Special scattering regimes for conical all-dielectric nanoparticles, *Sci. Rep.* **12**, 21904 (2022).
- [50] M. V. Rybin, K. L. Koshelev, Z. F. Sadrieva, K. B. Samusev, A. A. Bogdanov, M. F. Limonov, and Y. S. Kivshar, High-Q supercavity modes in subwavelength dielectric resonators, *Phys. Rev. Lett.* **119**, 243901 (2017).
- [51] A. Canales, O. V. Kotov, B. Küçüköz, and T. O. Shegai, Self-hybridized vibrational-mie polaritons in water droplets, *Phys. Rev. Lett.* **132**, 193804 (2024).
- [52] E. A. Muljarov and W. Langbein, Comment on “Normalization of quasinormal modes in leaky optical cavities and plasmonic resonators”, *Phys. Rev. A* **96**, 017801 (2017).
- [53] G. B. Arfken and H. J. Weber, *Mathematical Methods for Physicists*, 6th ed. (Elsevier, London, 2011).
- [54] E. A. Muljarov, W. Langbein, and R. Zimmermann, Brillouin-Wigner perturbation theory in open electromagnetic systems, *Europhys. Lett.* **92**, 50010 (2010).
- [55] R. Alaei, C. Rockstuhl, and I. Fernandez-Corbaton, An electromagnetic multipole expansion beyond the long-wavelength approximation, *Opt. Commun.* **407**, 17 (2018).
- [56] S. Gladyshev, O. Pashina, A. Proskurin, A. Nikolaeva, Z. Sadrieva, M. Petrov, A. Bogdanov, and K. Frizyuk, Fast simulation of light scattering and harmonic generation in axially symmetric structures in comsol, *ACS Photonics* **11**, 404 (2024).
- [57] H. S. Sehmi, W. Langbein, and E. A. Muljarov, Optimizing the Drude-Lorentz model for material permittivity: Method, program, and examples for gold, silver, and copper, *Phys. Rev. B* **95**, 115444 (2017).
- [58] Optical Data from Sopra SA - GaAs (Gallium Arsenide) (2008), online.
- [59] S. V. Zhukovsky, A. Andryieuski, O. Takayama, E. Shkondin, R. Malureanu, F. Jensen, and A. V. Lavrinenko, Experimental demonstration of effective medium approximation breakdown in deeply subwavelength all-dielectric multilayers, *Phys. Rev. Lett.* **115**, 177402 (2015).
- [60] C. F. Bohren and D. R. Huffman, *Absorption and Scattering of Light by Small Particles*, 6th ed. (John Wiley & Sons, New York, 1983).
- [61] J. C. Lagarias, J. A. Reeds, M. H. Wright, and P. E. Wright, Convergence properties of the nelder-mead simplex method in low dimensions, *SIAM J. Optim.* **9**, 112 (1998).
- [62] Broyden–Fletcher–Goldfarb–Shanno algorithm - Wikipedia, [Online].